Applied Microbiology and Biotechnology (2021) 105:1051–1062
https://doi.org/10.1007/s00253-020-11079-9

BIOTECHNOLOGICAL PRODUCTS AND PROCESS ENGINEERING

High density fermentation of probiotic *E. coli* Nissle 1917 towards heparosan production, characterization, and modification

Payel Datta[1] · Li Fu[1] · Paul Brodfuerer[1] · Jonathan S. Dordick[1,2] · Robert J. Linhardt[1,2,3]

Received: 5 October 2020 / Revised: 18 December 2020 / Accepted: 27 December 2020 / Published online: 22 January 2021

Abstract

Heparosan is a naturally occurring non-sulfated glycosaminoglycan. Heparosan serves as the substrate for chemoenzymatic synthesis of biopharmaceutically important heparan sulfate and heparin. Heparosan is biologically inert molecule, non-toxic, and non-immunogenic and these qualities of heparosan make it an ideal drug delivery vehicle. The critical-to-quality (CTQ) attributes for heparosan applications include composition of heparosan, absence of any unnatural moieties, and heparosan molecular weight size and unimodal distribution. Probiotic bacteria *E. coli* Nissle 1917 (EcN) is a natural producer of heparosan. The current work explores production of EcN heparosan and process parameters that may impact the heparosan CTQ attributes. Results show that EcN could be grown to high cell densities (OD_{600} 160–180) in a chemically defined media. The fermentation process is successfully scaled from 5-L to 100-L bioreactor. The chemical composition of heparosan from EcN was confirmed using nuclear magnetic resonance. Results demonstrate that heparosan molecular weight distribution may be influenced by fermentation and purification conditions. Size exclusion chromatography analysis shows that the heparosan purified from fermentation broth results in bimodal distribution, and cell-free supernatant results in unimodal distribution (average molecular weight 68,000 Da). The yield of EcN-derived heparosan was 3 g/L of cell free supernatant. We further evaluated the application of Nissle 1917 heparosan for chemical modification to prepare *N*-sulfo heparosan (NSH), the first intermediate precursor for heparin and heparan sulfate.

Key points

- *High cell density fermentation, using a chemically defined fermentation media for the growth of probiotic bacteria EcN (E. coli Nissle 1917, a natural producer of heparosan) is reported.*
- *Process parameters towards the production of monodispersed heparosan using probiotic bacteria EcN (Nissle 1917) has been explored and discussed.*
- *The media composition and the protocol (SOPs and batch records) have been successfully transferred to contract manufacturing facilities and industrial partners.*

Keywords Chemoenzymatic modifications · EcN · *E. coli* Nissle 1917 · *E. coli* K5 · Fed-batch fermentation · Heparin · Heparan sulfate · Heparin lyase · Heparosan · High cell density fed-batch fermentation · Probiotic Nissle 1917 · *N*-sulfo heparosan

✉ Jonathan S. Dordick
dordick@rpi.edu

✉ Robert J. Linhardt
linhar@rpi.edu

[1] Center for Biotechnology and Interdisciplinary Studies, Rensselaer Polytechnic Institute, Troy, NY 12180, USA

[2] Department of Chemical and Biological Engineering, Rensselaer Polytechnic Institute, Troy, NY 12180, USA

[3] Department of Chemistry and Chemical Biology, Rensselaer Polytechnic Institute, Troy, NY 12180, USA

Introduction

Heparosan (*N*-acetyl heparosan) is a polydisperse, linear glycosaminoglycan. This polysaccharide has a homogeneous structure comprised of [→4) β-D-glucuronic acid (GlcA) (1→4) *N*-acetyl-α-D-glucosamine (GlcNAc) (1→]$_n$ repeating disaccharide units (Zhang et al. 2010). Heparosan is found in certain bacteria (e.g., *Escherichia coli* K5 and *Pasteurella multocida*), and also serves as a precursor backbone in the eukaryotic biosynthesis of heparan sulfate (Vann et al. 1981; DeAngelis and White 2002; Linhardt and Toida 2004;

Wang et al. 2010). In bacteria, capsular polysaccharides (such as heparosan) may aide in survival and biofilm formation, and protect the bacteria from host immune system (Linhardt and Toida 2004). Heparosan is also a biologically inert molecule, non-toxic, and non-immunogenic, and these qualities of heparosan make it an ideal drug delivery vehicle (Deangelis 2015; Qiu et al. 2019; Rippe et al. 2019). Heparosan, derived from microbial sources such as *E. coli* K5, has been successfully used for the chemoenzymatic synthesis of biosynthetic heparan sulfates and heparin (Lindahl et al. 2005; Fu et al. 2016). Heparan sulfate is a biologically important glycosaminoglycan involved in angiogenesis, cell growth, cell signaling, developmental biology, inflammation, anticoagulation, and in viral, bacterial and parasitic infection (Lindahl et al. 1998; Linhardt and Toida 2004). Heparin, a highly sulfated analog of heparan sulfate, is an important anticoagulant drug (8). Pharmaceutical heparin is generally derived from animal-sourced porcine intestinal mucosa (Linhardt 2003). Animal-sourced heparin can contain virus, prion, and process impurities and has been known to contain contaminants and adulterants (Linhardt 2003). The production of biosynthetic heparins using chemoenzymatic processes offers a potentially safer route for heparin production (Xu et al. 2011; Liu and Linhardt 2014; Fu et al. 2016; Zhang et al. 2020; Wang et al. 2020).

E. coli Nissle 1917 produces heparosan and is a biosafety level I (BSL-1) organism that is commercially used as a probiotic nutraceutical. The genomes of *E. coli* K5 and Nissle 1917 have been sequenced (Cress et al. 2013a; Cress et al. 2013b). Both *E. coli* K5 and *E. coli* Nissle 1917 express the *E. coli* Group 2 capsule K5 gene cassette (Cress et al. 2013a; Cress et al. 2013b; Cress et al. 2014), which encodes genes that are critical for heparosan production (synthesis and export) (Fig. 1) (Cress et al. 2013a; Cress et al. 2013b; Cress et al. 2014). Glycosyltransferases KfiABCD (KfiA, KfiB, KfiC, and KfiD, encoded by genes in region 2) are responsible for biosynthesis of the heparosan chain. The heparosan chain is then exported to the cell surface through the action of the heparosan transport proteins KpsFEDUCS (KpsF, KpsE, KpsD, KpsU, KpsC, and KpsS, encoded by genes in region 1), and KpsMT (KpsM, and KpsT encoded by genes in region 3) (Cress et al. 2014). In parallel, gene regulation may play an important role expression of KfiABCD, KpsFEDUCS, and KpsMT. For example, transcriptional regulators such as RFAH, SlyA, and H-NS may regulate the expression of heparosan production (Rowe et al. 2000; Corbett et al. 2007; Xue et al. 2009; Yan et al. 2015). Growing *E. coli* K5 cells are also known to shed the heparosan into the supernatant during high-cell density fermentations (Wang et al. 2010).

The current study explores high cell density fermentation of *E. coli* Nissle 1917 using a chemically defined media. A chemically defined media refers to a fermentation media that is not complex and does not contain yeast extract, tryptone, or peptone. In addition, the study focuses on characterization of *E. coli* Nissle derived heparosan. The critical-to-quality attribute (CTQ) for heparosan applications includes the sameness of heparosan and its disaccharide building blocks, absence of unnatural building blocks, heparosan chain length (MW), and heparosan chain dispersity. While heparosan yield is important, the low cost of fermentation media and the ability to produce heparosan in a BSL-1 rather than a BSL-2 facility, have a major impact in reducing heparosan production costs. Moreover, a heparosan nutraceutical from a non-genetically modified organism (GMO), the non-pathogenic *E. coli* Nissle 1917 strain, might be of particular value for the more restricted European market. Another potential application is the use of heparosan as an inert drug delivery vehicle (6). A key need for commercial application, therefore, is the high cell density fermentation of *E. coli* Nissle 1917 using a chemically defined media to obtain high titers of heparosan and production of heparosan that meet CTQ attributes.

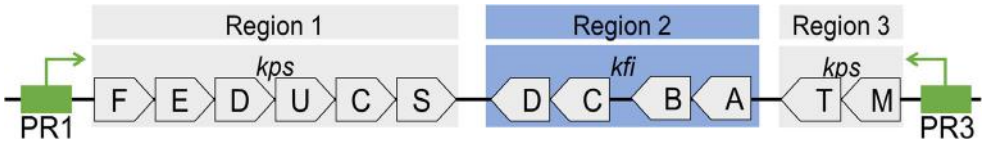

Fig. 1 The *E. coli* group 2 capsular K5 gene cluster are present in both *E. coli* K5 and *E. coli* Nissle chromosome. The products of the gene cluster are involved in heparosan production (biosynthesis and export). The region 2 (kfi *ABCD*) is serotype specific and encodes for gene-products (kfiA, kfiB, kfiC, and kfiD) that are responsible for heparosan biosynthesis. The region 1 (kps *FEDUCS*), and region 3 (kps *MT*) are conserved across *E. coli* expressing group 2 capsules and are responsible for heparosan export, including (1) KDO biosynthesis (kpsF and kpsU), (2) translocation across cytoplasmic membrane (kpsC, kpsS, and kpsMT), and (3) translocation across periplasm and outer membrane (KpsD and KpsE). Upstream promoter regions (PR1–3) promote the binding of RNA polymerase and initiate transcription. In bacteria, the promoter regions may be regulated through actions of activator and repressor proteins. For example, the kps gene cluster is temperature-controlled; H-NS and BipA may promote maximal transcription at 37 °C and transcription repression at 20 °C. In addition, antitermination transcription factor (e.g., RfaH) may aide in upregulation of heparosan production. It should be noted that though both *E. coli* K5 and Nissle express the capsular K5 gene cluster, and there might be differences in expression, including the transcription regulators

Materials and methods

Chemicals

All chemicals were purchased from Sigma-Aldrich (St. Louis, MO, USA) or GenScript (Piscataway, NJ), ThermoFisher Scientific (Waltham, MA), and GoldBio. (St Louis MO). Disaccharide standards were purchased from Iduron (Manchester, UK).

Heparosan production in 5-L and 100-L bioreactor

The heparosan fermentations (*E. coli* K5 and Nissle 1917) consisted of a batch phase, followed by a fed-batch phase. The seed media and batch media are chemically defined media and consist of glucose (18–20 g/L), potassium phosphate monobasic (13.5 g/L), ammonium phosphate (4.0 g/L), magnesium sulfate heptahydrate (1.4 g/L), citric acid (1.7 g/L), and trace metals solution (10.0 ml/L). The pH was adjusted to 6.8 ± 0.05. The composition of trace metals solution is provided in supplement information Table S1. The batch phase was initiated with the inoculation of seed culture in batch media (starting OD_{600} = 0.25 ± 0.1). In certain fermentations (e.g., 100-L scale), a seed train was used before inoculating into the fermentor. A typical seeding strategy consisted of the following steps, (1) starter culture: seeding 100–200 μl glycerol stock to two to five 50–100 mL flask and cells incubated at 220 rpm for 8–12 h at 37 °C, (2) stage 1 seed flask: starter culture (10–15 ml) was added to two to five stage 1 seed flasks, and cells incubated at 220 rpm for 8–12 h at 37 °C, (3) stage 2 seed flasks: stage 1 seed flask (50–150 ml) was added to 5–8 stage 1 seed flasks, and cells incubated at 37 °C at 220 rpm for 4–8 h. Alternatively, overnight cultures (seed 1) were inoculated in seed 2 and the cells were grown to a cell density (OD_{600}) of 4.0–6.0. The cells were inoculated (5–10% by vol) in batch media. For example, for a 100-L bioreactor, a typical 50-L batch media inoculation uses 5-L media from stage 2 seed flasks. The fermentation was maintained at 37 °C, and pH was set at 6.8 ± 0.05. The fermentation and bioreactor conditions are provided in supporting Table S2. Feed was initiated when the pH increases from 6.8 ± 0.05 to 7.0 ± 0.05. In some experiments, feed was initiated when (OD_{600}) reached 8.0 ± 2.5. The cells were fed with a concentrated glucose feed (700 g/L glucose, supplemented with 10 g/L magnesium sulfate heptahydrate, 47 g/L potassium phosphate monobasic, 0.4 g/L thiamine-HCl, and 20 ml/L trace metals solution). The feed rate was adjusted, based on fluctuations in glucose level, pH, and dissolved oxygen (DO) levels. If required, the concentrated feed may be stopped intermittently to exhaust the glucose and feed re-initiated when the pH increased from 6.8 ± 0.05 to 7.0 ± 0.05. In certain experiments, glucose in seed media, batch media, and feed were replaced with glycerol. The fermentation was stopped when the OD_{600} reached 140 ± 20. The fermentation broth was centrifuge at 13,000×*g* for 45 min/4 °C to separate cells and supernatant. The cell-free supernatant was stored in − 20 °C and used for heparosan purification. In certain experiments, the fermentation broth was autoclaved and used for heparosan purification.

Heparosan purification

Heparosan was purified from cell-free supernatant or autoclaved fermentation broth using a previously described method (Wang et al. 2011) with some modification. Briefly, the cell-free supernatant or autoclaved fermentation broth was transferred to a clean glass beaker with stirrer. The experiment was performed in chemical hood. A solution of sodium hypochlorite (NaClO) was added slowly to the stirred supernatant or autoclaved fermentation broth till a final concentration of 1–6% of the total volume. The solution was incubated at 22 ± 3 °C for 16–24 h, with stirring (100–1000 rpm). The solution was transferred to a clean centrifuge bottle and centrifuged at 12,000× *g*/22 ± 3 °C for 20 min. The supernatant was collected and transferred to a clean glass beaker with stirrer. The supernatant was mixed with equal volume of 100% isopropanol and incubated at 22 ± 3 °C for 1 h, with constant stirring. The solution was centrifuged at 12,000×*g*/22 ± 3 °C for 20 min, and heparosan pellet was collected. The heparosan pellet is washed multiple times with 60% isopropanol/water using centrifugation (12,000×*g*/22 ± 3 °C for 20 min). Final wash of the heparosan pellet is performed with SDA-3C ethanol and centrifugation at 12,000×*g*/22 ± 3 °C for 20 min. The heparosan pellet is dried using vacuum at 40 °C. The heparosan pellet is dried overnight and until a constant weight is reached as determined by two consecutive weight measurements (variations within 0.05 g of each other).

Conversion of heparosan to NSH

The chemical conversion of *E. coli* K5 and Nissle-derived heparosan was performed using a previously described method (Wang et al. 2011) with some modifications. Briefly, heparosan was purified from cell-free supernatant and dried using vacuum (16 h/40 °C). The dried heparosan (1.00 g) was dissolved in DI water (6.5 mL) at 60 °C. The heparosan solution was diluted with 2 N NaOH, a 1% heparosan solution in 1.0 N NaOH. The 1% heparosan solution was stirred at 53 °C for 20–25 h, then cooled to 10 °C, and neutralized with conc. HCl to pH 6.5. Na_2CO_3 (1.50 g, 14.1 mmol) and $NMe_3.SO_3$ (1.50 g, 10.8 mmol) were added. The resulting mixture was stirred at 47 °C for 48 h, and then cooled to 30 °C. The crude NSH was precipitated with addition of an equal volume of SDA-3C ethanol. The mixture was centrifuged (12,000×*g*/22 ± 3 °C for 20 min), and the supernatant discarded. The pellet was washed thrice with 60% SDA-3C ethanol/water

(10–15 mL) and dried to constant weight under vacuum at 40 °C. The NSH was analyzed for recovery yield, and MW. In addition, % NS and % free amine were analyzed using previously described disaccharide analysis (Zhao et al. 2012; Zhao et al. 2013) and OPA assays (Yang et al. 2011), respectively.

1D 1H nuclear magnetic resonance (NMR)

Heparosan and NSH samples were analyzed using 1D 1H nuclear magnetic resonance (NMR) and with the conditions as previously described (Fu et al. 2017). Briefly, the purified samples (each 1.5 mg) were dissolved in 0.5 mL D_2O (99.996%, Sigma Aldrich, St. Louis, MO, USA). The samples were lyophilized and re-dissolved in D_2O, and the process was performed multiple times for complete deuterium–hydrogen exchange. For the NMR analysis, the samples were dissolved in 0.4 mL 99.996% D_2O and 1H-NMR spectra were acquired using a Brüker Ultrashield 600 MHz (14.1 Tesla) NMR instrument.

Size exclusion chromatography (SEC)

The molecular weight of heparosan and NSH were performed using size exclusion chromatography (SEC) and with the conditions as previously described (Wang et al. 2011). Briefly, purified samples (weighed 5 mg) were dissolved in HPLC grade water (1 mL). The samples were analyzed using a TSK-GEL G3000PWxl size exclusion column with a sample injection volume of 20 μl and a flow rate of 0.6 ± 0.1 mL/min with a SEC apparatus that comprised of a Shimadzu LC-10Ai pump, a Shimadzu CBM-20A controller, and a Shimadzu RID-10A refractive index detector. The SEC chromatograms were recorded and analyzed with "GPC Postrun" function to calculate MN and MW. Molecular weight data was measured with heparin reference standards.

Disaccharide compositional analysis

The disaccharide composition analysis of heparosan and NSH was performed using a high-pressure liquid chromatography (HPLC)—ultraviolet spectrometry (UV) and with the conditions as previously described (Fu et al. 2017). Heparosan and NSH samples (200 μg each) were completely digested with heparin lyase I, II, and III (10 mU each) in 200 μL 50 mM ammonium acetate buffer (pH 7.2) at 37 °C for 12 h. The resulting disaccharides were purified and analyzed using a high-pressure liquid chromatography (HPLC)—ultraviolet spectrometry (UV). The chromatograms were analyzed using disaccharide standards (purchased from Iduron).

Fed-batch fermentation and purification of analytical enzymes (heparin lyases)

Analytical enzymes are used for disaccharide analysis of heparosan and NSH. Recombinant *E. coli* BL21 strains expressing either heparin lyase 1, 2, or 3 were produced using fed-batch fermentation. The fed-batch fermentation and purification for heparin lyase 3 has been previously described (Datta et al. 2020). The media composition (seed, batch, feed), and fermentation conditions for heparin lyase 1 and 2 are similar to heparin lyase 3 (Table S3).

Data analysis

All data analysis was performed using BioRad Image Lab software, Microsoft Excel, GraphPad Prism 8 (GraphPad, San Diego, CA), and Python 3.9 (https://www.python.org/).

Results

Cell growth of *E. coli* Nissle 1917 (EcN) using a chemically defined media and fed-batch fermentation

The first focus was defining the parameters for achieving cell growth of *E. coli* Nissle 1917 using a chemically defined media that lack any complex chemicals and animal-sourced components, including peptone, tryptone, or yeast extract. The experiment was performed using a 5-L bioreactor. The aim of the experiments was to answer specific questions, including (1) growth of *E. coli* Nissle using chemically defined media, (2) calculate the volume of starting batch media vs. final fermentation broth, and (3) heparosan production. As a starting point, specific fermentation parameters were selected based on the genetics of the bacteria. For example, the fermentation temperature was maintained at 37 °C, as the transcription of heparosan production enzymes may be directly or indirectly regulated by proteins, including H-NS and BipA, wherein both H-NS and BipA promote maximal transcription at 37 °C and transcriptional repression at 20 °C (Rowe et al. 2000; Corbett et al. 2007; Xue et al. 2009). Specific parameters were selected based on *E. coli* K5 fermentation (Wang et al. 2010). These parameters include pH (set at 6.8) and dissolved oxygen (set at 20–30%). These parameters could be further explored to optimize heparosan production in *E. coli* Nissle. Gram-negative *E. coli* K5 expresses the genes required for heparosan production and is capable of producing heparosan when grown on both glucose and glycerol (Wang et al. 2014; Yamazaki et al. 2020). The first set of experiments explored fed-batch fermentations of *E. coli* Nissle 1917 using either of glucose or glycerol as carbon source. Ammonium hydroxide was used as the nitrogen source. A chemically defined formulation was used for seed batch and feed. Overnight

cultures (12–16 h) were inoculated (5–10% by vol) from shake flasks in the batch media, and when the cell growth (OD_{600}) reached 8.0 ± 2.5, feeding was initiated. Results show that *E. coli* Nissle 1917 cells could grow in a chemically defined glucose-media and reach a final OD_{600} > 100 (Fig. S1). A 2.5-L starting batch media, at the end of fermentation, resulted in ~4-L culture volume, with ~0.7–0.8 L feed consumed, and 0.5–0.8 L base (5 M NH_4OH) consumed. For a detailed heparosan study, at least 10–100 g heparosan is required, and so the next question we asked was the yield of heparosan from Nissle fermentation and the scale needed to produce 10–100 g heparosan. The fed-batch fermentation with glycerol as sole carbon source was also explored and may require additional optimization experiments. However, we suggest that high cell density fermentations of *E. coli* Nissle 1917 may be achieved using glycerol defined media with some minor fermentation modifications.

Defining the parameters for purification of heparosan from *E. coli* Nissle 1917

Heparosan is produced inside the cells, exported to the cell surface, and shed into the supernatant. We next focused on heparosan purification strategies and the heparosan chain polydispersity obtained from both fermentation broth (cells and fermentation supernatant) and cell-free supernatant. Heparosan was purified from fermentation broth and cell-free supernatant, using IPA purification, and analyzed for MW and chain polydispersity.

There are various analytical methods to evaluate MW of heparosan, including gel electrophoresis, capillary electrophoresis, and size exclusion chromatography (Ly et al. 2011; Restaino et al. 2019). For the current study, the size exclusion chromatography (SEC-HPLC) method was chosen to evaluate the MW and polydispersity of heparosan. SEC-HPLC has been used for the evaluation of animal-sourced heparin (Zhang et al. 2011). *E. coli* derived heparosan may be used as the substrate for biosynthetic heparin. The use of a similar MW analysis method may in part facilitate the analysis (e.g., changes in MW and polydispersity during the chemoenzymatic synthesis of heparin from heparosan). Results demonstrated that heparosan from fermentation broth showed a bimodal chain distribution (Fig. 2). We hypothesize that the total heparosan in the fermentation broth may be a mixture of growing heparosan chains within the cells and shed heparosan in the supernatant and therefore, results in a heparosan product having a mixture of chain lengths, with both a relatively high molecular weight and a high polydispersity. Next, the fermentation broth was centrifuged, and cell-free supernatant was obtained. Heparosan obtained from the cell-free supernatant had a relatively high MW and a unimodal chain distribution (Fig. 2). A unimodal molecular weight distribution of heparosan chains is desirable as it represents a more homogenous product for applications including (1) substrate for chemoenzymatic synthesis of heparan sulfate and heparin, (2) inert drug vehicle, and (3) nutraceutical. It should be noted that the heparosan may contain process impurities, such as nucleic acids, proteins, lipopolysaccharides, endotoxins, and metals. One of the future objectives of the project includes evaluation and removal of process impurities.

High cell density fermentation of *E. coli* Nissle 1917 (EcN)

Characterization, modification, application, and analysis of heparosan would require 10–100 g heparosan. Next, *E. coli*

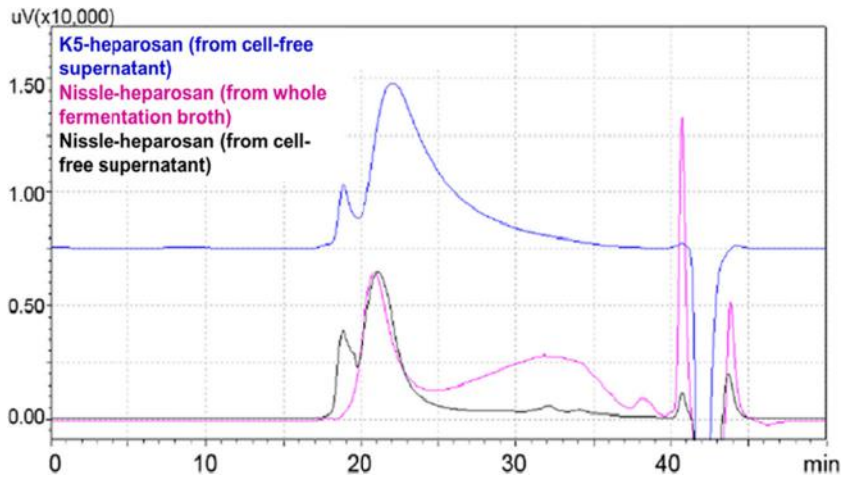

Fig. 2 Heparosan production in *E. coli* Nissle 1917 (EcN). Heparosan was purified from fermentation broth and cell-free supernatant and analyzed using GPC. Heparosan isolated from cell-free supernatant of *E. coli* K5 was used as the positive control. The *x*-axis denotes MW distribution (from higher to lower MW). The area under the curve of the histogram denotes heparosan chain distribution. Using different concentrations of heparin, the concentration under the curve could be calculated. Results demonstrate that heparosan from cell-free supernatant from *E. coli* K5 and *E. coli* Nissle have similar molecular weight distribution

Nissle (EcN)-derived heparosan was produced using the chemically defined media and a fed-batch feeding strategy. Results demonstrate that *E. coli* Nissle biomass could be successfully grown to cell densities of OD_{600} 8–12 (3.3 ± 0.9 g/L DCW) in a chemically defined media in batch fermentation mode. Figure 3 demonstrates the representative fermentation profile of increased biomass with time. The fermentation was maintained at 37 °C. At the end of the fermentation (t = 40–45 h) the cell density was OD_{600} = 135 (44.55 ± 1.35 g/L DCW). Production of high cell density biomass required a controlled fed-batch fermentation approach, including (1) feeding strategy (Fig. 4) and (2) maintaining the oxygen demand of the growing biomass (Fig. 5).

To achieve high cell density requires feeding the cells with concentrated feed. The concentrated feed may be composed of carbon source (e.g., glucose), nitrogen source, and other essential metals. A concentrated glucose feed (supplemented with magnesium sulfate, potassium phosphate, and trace metals) was used for high cell density fermentation of *E. coli* Nissle fermentation. However, the uncontrolled addition and consumption of glucose feed may result in adverse effects. For example, it has been shown that glucose can affect heparosan production through the cyclic AMP (cAMP)—cAMP receptor protein (CRP) complex pathway (Yan et al. 2015). Moreover, excess carbon influx may result in the acetate build-up during aerobic fermentation. It has been demonstrated that acetate accumulations greater than 5 g L^{-1} affect *E. coli* K4 growth rates (Restaino et al. 2011). One of the approaches to control acetate accumulations in high cell density fermentations includes glucose-limited fed-batch fermentations that result in cell growth below the specific growth rate (Lee 1996; Phue and Shiloach 2004). Figure 4 shows the glucose feeding strategy used for fed-batch fermentation of *E. coli* Nissle 1917. The glucose level and pH were monitored and recorded during the fermentation (Fig. 4). The feed was initiated 5–8 h EFT, and once the glucose (initial concentration 18–20 g/L in the batch media) was exhausted, the glucose level was maintained at > 1–2 g/L. The pH was maintained at 6.71 ± 0.04 using 5 M NH_4OH. The NH_4OH served as the base to maintain the pH and the nitrogen source during the high cell density fermentation. This facilitates avoiding complex nitrogen sources (e.g., tryptone and peptone) and thereby lowering the cost of fermentation.

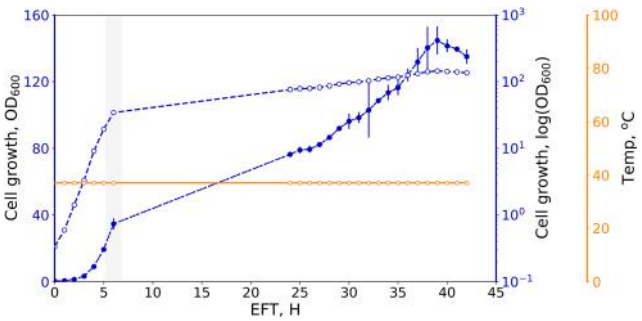

Fig. 3 Biomass growth of *E. coli* Nissle 1917 (EcN). The primary y-axis (blue dashed line) denotes cell growth, using offline OD_{600} spectrophotometer measurement (where, error bars denote, mean ± S.E., where n = 2 readings). The first secondary y-axis (blue dotted line) denotes cell growth represented as log (OD_{600}). The second secondary y-axis (orange line) denotes the fermentation temperature (°C). The vertical gray bar line on the x-axis denotes onset of fed-batch fermentation. Each mark on each line denotes data collection point. The graph demonstrates that a high cell density fermentation was achieved using a fed-batch fermentation approach and at the end of the fermentation (t = 40–45 h) the cell density reached OD_{600} = 135 (44.55 ± 1.35 g/L DCW). The fermentation was maintained at 37 °C

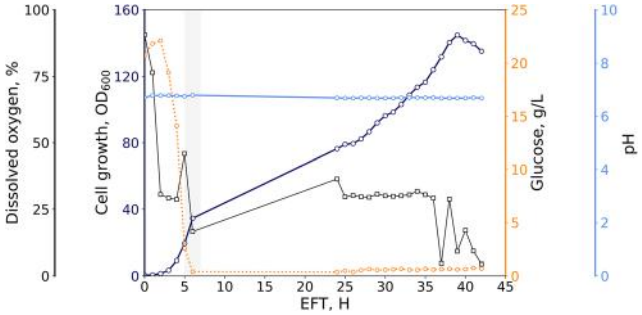

Fig. 4 High cell density fermentation of *E. coli* Nissle 1917 (EcN) using a glucose-limited fed-batch fermentation approach. The first primary y-axis (blue line) denotes cell growth, using offline OD_{600} spectrophotometer measurement. The second primary y-axis (black line) denotes dissolved oxygen (DO, %) measurements. The first secondary y-axis (orange dotted line) denotes glucose (g/L) in the fermentation broth. The second secondary y-axis (light blue line) denotes pH measurements. The vertical gray bar line on the x-axis denotes onset of fed-batch fermentation. Each mark on each line denotes data collection point. The glucose concentration was monitored, and the feed rate was adjusted to maintain low glucose-level in the fermentation broth. Results shows the glucose feeding strategy used for fed-batch fermentation of *E. coli* Nissle 1917, where, the feed was initiated 5–8 h EFT, and once the glucose (initial concentration 18–20 g/L in the batch media) was exhausted, the glucose level was maintained at > 1–2 g/L. The pH was maintained at 6.71 ± 0.04 using 5 M NH_4OH

High cell density aerobic fermentations require a steady supply of oxygen. With the increasing biomass growth, the microorganism oxygen demand increases and is characterized as the volumetric oxygen uptake rate (OUR, eq. 1).

$$OUR = Q_{O2}\, X \quad (1)$$

where

Q_{O2} = specific respiration (oxygen uptake) rate, mmoles O_2/g biomass h^{-1}

X = biomass concentration, g L^{-1}

The bioreactor design aims to ensure a steady supply of oxygen to the growing biomass and is characterized as the volumetric oxygen transfer rate (OTR). When OUR > OTR, the growth of the biomass may decrease or cease. The OTR is proportional to the volumetric oxygen mass transfer coefficient (K_La). The K_La (h^{-1}) is defined as the efficiency with which the oxygen is supplied into a bioreactor under specific defined parameters or conditions, including impeller design

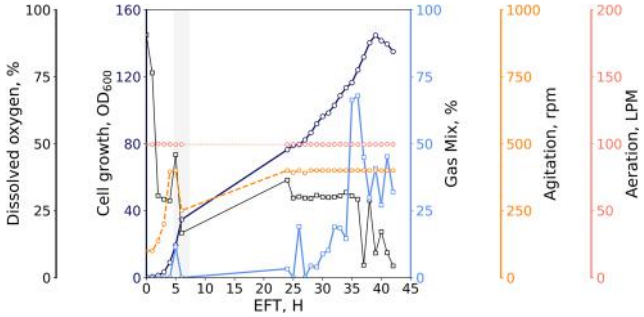

Fig. 5 High cell density fermentation of *E. coli* Nissle 1917 (EcN) using a glucose-limited fed-batch fermentation approach. The first primary y-axis (blue line) denotes cell growth, using offline OD_{600} spectrophotometer measurement. The second primary *y*-axis (black line) denotes dissolved oxygen (DO, %) measurements. The first secondary *y*-axis (blue line) denotes gas mix (%). The second secondary *y*-axis (orange dashed line) denotes agitation (rpm). The third secondary *y*-axis (pink dotted line) denotes aeration (slpm). The vertical gray bar line on the *x*-axis denotes onset of fed-batch fermentation. Each mark on each line denotes data collection point. The dissolved oxygen was set at 30% dissolved oxygen level. Results show with increasing biomass, the dissolved oxygen gradually decreased to below 30%. The oxygen demand during batch and fed-batch phases was maintained at 30% by controlling agitation (100–400 rpm) and providing a supply of gas mixture (0–90%). The agitation (mixing) was increase from 100 to 400 rpm during the batch and the fed-batch fermentation. The aeration was maintained at 99.5 ± 0.14 slpm. The fermentation was stopped when the change in OD_{600} over time indicated that the culture had entered stationary phase ($OD_{600} > 150$)

and agitation rate. The K_La is influenced by fermentation conditions, including (1) temperature, (2) aeration, (3) mixing time, (4) viscosity of the media, due to the addition of concentrated feed, growing biomass, and accumulation of extracellular products, and (5) specific media components, such as antifoam (Meyer et al. 2016). Both batch and fed-batch phase of the fermentation, the temperature was set at 37 °C and aeration at 100 slpm (Fig. 3 and Fig. 5). The agitation (mixing) was increase from 100 to 400 rpm during the batch and the fed-batch fermentation (Fig. 5). Maintaining a steady supply of oxygen during high cell density aerobic fermentation is critical for increasing the biomass and product formations. A low oxygen level may result in the accumulation of metabolites and may affect cell health and product formation (Restaino et al. 2011). The oxygen demand for *E. coli* Nissle fermentation was maintained at 30% dissolved oxygen level. Results (Fig. 5) show that with increasing biomass, the dissolved oxygen gradually decreased to below 30% (DO set point). The oxygen demand during fed-batch phase, when the cell density (biomass) gradually increased, was maintained at 30% by controlling agitation (100–400 rpm) and providing a supply of gas mixture (0–90%). The aeration was maintained at 99.5 ± 0.14 slpm. Fermentation temperature was maintained at 37 °C. Antifoam was supplied intermittently to control foaming during fermentation. The fermentation was stopped when the change in OD_{600} over time indicated that the culture had entered stationary phase ($OD_{600} > 150$).

E. coli Nissle 1917 (EcN) derived heparosan: purification and characterization

In post-fermentation, the supernatant was collected using batch centrifugation. The cell-free supernatant was used for heparosan isolation, characterization, and modifications. The Nissle-derived heparosan was evaluated for chemical composition and absence of unnatural moieties (NMR and disaccharide analysis), and intact chain size characterization (size exclusion chromatography). Heparosan derived from *E. coli* K5 was used as the positive control. *E. coli* K5 and Nissle 1917 fermentations were performed using a 100-L bioreactor and heparosan was purified from the cell-free supernatant. NMR and disaccharide analysis showed that both heparosan from *E. coli* K5 and *E. coli* Nissle 1917 were identical and absence of unnatural moieties (Fig. 6 and Table 1). The average molecular weight of heparosan from *E. coli* Nissle 1917 was slightly higher than the heparosan from *E. coli* K5 (Table 2). The heparosan yield was calculated using a size exclusion chromatography. Preliminary results showed that the purification method used in this paper may interfere with the conventional carbazole assay quantification. Based on the size exclusion chromatography method, and with similar fermentation and purification conditions, the yield of heparosan from *E. coli* Nissle 1917 is 3 g/L fermentation supernatant (Table S4). The yield of heparosan is being reported as g/L of supernatant instead of conventionally used g/DCW (to facilitate easier conversions for downstream calculations).

Modifications of *E. coli* Nissle 1917 (EcN)-derived heparosan: towards potential applications

The Nissle-derived heparosan can be successfully chemically modified to produce lower MW heparosan. Both higher and lower MW Nissle-derived heparosan can be successfully modified to crude NSH and purified NSH (Table S5, Table S6, and Table 3). Briefly, heparosan purified from cell-free supernatant from both *E. coli* K5 and Nissle 1917 can be successfully converted to crude NSH (under dilute 1% reaction conditions) (Table S6) and further purified to NSH (Table 3), affording similar percentage of *N*-sulfated disaccharide sequences (% NS) and a similar molecular weight and polydispersity index.

Discussion

Heparosan is a naturally occurring non-sulfated glycosaminoglycan. Heparosan is a linear polysaccharide composed of alternating glucuronic acid (GlcA) and *N*-acetyl glucosamine (GlcNAc). Heparosan is biopharmaceutically important chemicals and serves as the substrate for the chemoenzymatic synthesis of heparan sulfates and heparin (Linhardt et al. 2007;

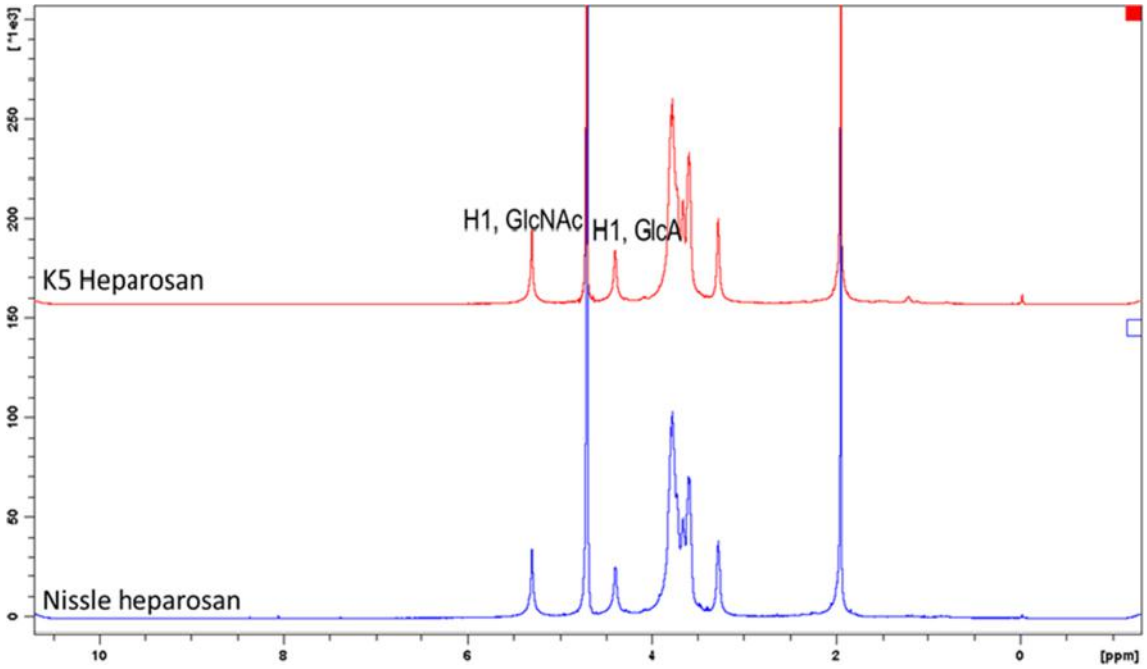

Fig. 6 Chemical composition analysis of heparosan using 1H-NMR. The chemical composition analysis of heparosan from *E. coli* Nissle was performed using 1H-NMR. Heparosan from *E. coli* K5 was used as the positive control. Results demonstrate that heparosan derived from *E. coli* K5 and Nissle 1917 are similar in composition

Kim et al. 2020). Other potential applications of heparosan include utilization of heparosan as an inert-drug or nutraceutical. The critical-to-quality (CTQ) attributes for heparosan applications are (1) composition of heparosan, (2) absence of any unnatural moieties, including sulfated GlcA and GlcNAc, and (3) heparosan molecular weight size and unimodal distribution. Probiotic bacteria *E. coli* Nissle 1917 (EcN) is a natural producer of heparosan to obtain high titers of heparosan and production of heparosan that meet CTQ attributes. The current work explores production of EcN heparosan and process parameters that may impact the heparosan CTQ attributes.

A key need for commercial application is the high cell density fermentation of *E. coli* Nissle 1917 using a chemically defined media. The current study demonstrates that high cell density fermentation of *E. coli* Nissle 1917 in a chemically defined medium results in heparosan production. Currently, the microbial production of heparosan has been successfully explored in naturally occurring bacteria (e.g., *E. coli* K5, *Pasteurella multocida*, and *E. coli* Nissle 1917) and in engineered *Bacillus sps.*, and *E. coli* BL21 strains (DeAngelis and White 2002; Wang et al. 2010; Zhang et al. 2012; Wang et al. 2014; Chen et al. 2017; Williams et al. 2019; Yamazaki et al. 2020). The reported yields of heparosan, using fed-batch fermentations, from natural producers and engineered strains range from 15 g/L (e.g., in *E. coli* K5) to 2.74 g/L (e.g., in engineered *Bacillus megatarium*) (Wang et al. 2010; Wang et al. 2014; Williams et al. 2019). However, under, specific experimental conditions (e.g., fermentation media, bioreactor conditions, purification method, and analysis method), the heparosan chain size, polydispersity, and yield from the naturally occurring and engineered strains may vary. For the current study, *E. coli* K5 and Nissle 1917 fermentation, purification, and characterization were performed with similar experimental conditions. The cell growth of Nissle 1917 was similar to *E. coli* K5, under similar fermentation conditions, with both fermentations reaching a harvest cell density (OD_{600}) of > 120 (Fig.

Table 1 *E. coli* Nissle 1917 (EcN)-derived heparosan disaccharide composition analysis shows presence of only unsulfated disaccharides building blocks (β-D-glucuronic acid and *N*-acetyl-α-D-glucosamine)

E. coli strain	Disaccharide compositional analysis Non-sulfated disaccharides ΔUA-GlcNAc
E. coli K5	100%
E. coli Nissle 1917 (EcN)	100%

Table 2 *E. coli* Nissle 1917 (EcN) derived heparosan intact chain characterization using size exclusion chromatography

E. coli strain	Intact chain characterization		
	MW (Da)	Mp	MW distribution
E. coli K5	58,400	78,400	Unimodal
E. coli Nissle 1917 (EcN)	68,000	89,000	Unimodal

S2). However, the colors of the cell-free supernatant of *E. coli* K5 and Nissle heparosan were different (Fig. S3). The Nissle-derived heparosan was evaluated for chemical composition and absence of unnatural moieties (NMR and disaccharide analysis), and intact chain size characterization (size exclusion chromatography). Heparosan was recovered from cell-free supernatant from *E. coli* Nissle 1917 (100-L fermentation). The supernatant was first treated with sodium hypochlorite to remove proteins and endotoxins (lipopolysaccharides, LPS) (Suwan et al. 2012). The main degradative effect of sodium hypochlorite treatment is the desired scission of the high MW heparosan to lower MW distribution. There may be additional degradation, but this has not been studied. The heparosan was precipitated using isopropyl alcohol. The alcohol-precipitated heparosan was freeze-dried. The Nissle-derived heparosan was characterized and *E. coli* K5-derived heparosan (that has been successfully used for synthesis of heparin and heparan sulfates) was used as the positive control. NMR and disaccharide analysis showed that both heparosan from *E. coli* K5 and *E. coli* Nissle 1917 were identical and absence of unnatural moieties (Fig. 6 and Table 1). The average molecular weight of heparosan from *E. coli* Nissle 1917 was slightly higher than the heparosan from *E. coli* K5 (Table 2). These results suggest that *E. coli* Nissle 1917 heparosan could be substituted for *E. coli* K5-derived heparosan in most applications. The heparosan molecular weight (chain length) is a CTQ attribute for heparosan applications. The heparosan chain length can be reduced by chemical depolymerization under certain conditions to obtain a smaller average chain length. However, the depolymerization method used should not increase the polydispersity of the heparosan chain. In conclusion, the comparative characterization of heparosan from *E. coli* K5 and *E. coli* Nissle demonstrates that the resulting heparosan chains from both organisms are comprised of [→4) β-D-glucuronic acid (GlcA) (1→4) *N*-acetyl-α-D-glucosamine (GlcNAc) (1→]n repeating disaccharide units. The heparosan isolated from the cell-free supernatant has a unimodal MW distribution, suggesting that the heparosan chains are relatively homogenous in chain length (Fig. 2). The homogenous mixture of heparosan chain may be a desirable feature for downstream processing and applications, including chemoenzymatic synthesis of heparin (Zhang et al. 2011).

Potential applications of heparosan include (1) heparosan as an inert-drug or nutraceutical; and (2) chemoenzymatically modified to biosynthetic heparan sulfate. For example, the *E. coli* K5-derived heparosan has been successfully utilized for the chemoenzymatic synthesis of heparan sulfate (Linhardt et al. 2007). Differences in the heparosan chain length between *E. coli* K5 and Nissle 1917 (Table 2) led us to evaluate whether the difference in chain length might impact NSH synthesis. NSH is the first intermediate polysaccharide and acts as a precursor for biosynthetic heparan sulfate production (Wang et al. 2011). The biosynthesis of heparan sulfate is a non-template-driven process, and each biosynthetic enzyme relies on the availability of substrate-binding site on the intermediate polysaccharide chain (Wang et al. 2011; Datta et al. 2013; Fu et al. 2017; Zhang et al. 2020). The sulfation percentage and pattern on the intermediate polysaccharides have shown to dictate the enzymatic synthesis of heparan sulfate and heparin (Wang et al. 2011; Datta et al. 2013; Fu et al. 2017; Zhang et al. 2020). In parallel, the sulfation pattern on heparan sulfate can also impact its biological activity, including binding sites for fibroblast growth factors (FGFs) and glycoproteins involved in the blood coagulation cascade (i.e., antithrombin III) (Linhardt and Toida 2004; Soares da Costa et al. 2017; Zhang et al. 2020). Therefore, the successful conversion of heparosan to NSH is a critical parameter towards chemoenzymatic synthesis of heparan sulfate. The current work demonstrates that Nissle-derived heparosan can be successfully chemically modified during purification of heparosan step. The chemical modifications of heparosan resulted in lower MW heparosan. Both higher and lower MW Nissle-derived heparosan can be successfully modified to crude NSH and purified NSH that exhibit similar percentage of *N*-sulfated disaccharide sequences (% NS) and a similar molecular weight and polydispersity index (Table S5, Table S6, and Table 3). Preliminary results also show that the NSH synthesized from Nissle-derived heparosan can be successfully enzymatically modified using heparan sulfate biosynthetic enzymes. These results suggest that Nissle-derived heparosan could be an additional source of heparosan for the chemoenzymatic synthesis of biosynthetic heparan sulfates.

Future directions include process improvements and evaluation of product efficacy and safety. For example, cell lysis may be responsible for contamination and impurities of extracellular heparosan. Cell-associated impurities could be re-

Table 3 Chemoenzymatic modification of heparosan from *E. coli* Nissle 1917

Heparosan source	Input Heparosan		NSH conversion		
	MW	MW distribution	MW	% NS ΔUA-GlcNS	% free amine
E coli K5	58,400	Unimodal	20,700	85.7	0.1
E. coli Nissle 1917 (EcN)	68,000	Unimodal	29,800	96.2	0.1

duced or removed using strong anion exchange resins. Strong anion exchange resins are utilized by industry for other glycosaminoglycan purifications from animal sources (Zhang et al. 2011). The purity of heparosan is a critical factor for its safe and effective applications, including (1) as a nutraceutical and (2) substrate for biosynthetic heparan sulfate and heparin. Analysis of purity includes but is not limited to (1) analysis of the composition of the heparosan chain and absence of any unnatural moieties, and (2) analysis of process impurities and contaminants. The 1D1H NMR requires 99.99% pure heparosan solution and thus may serve as the first screening for heparosan purity. However, other undetected process impurities and contaminants should be evaluated, including lipopolysaccharide, protein, nucleic acids, and metals. For example, *E. coli*-derived heparosan may have process impurities, including, presence of 2-keto-3-deoxy-D-mannooctulonic acid (KDO) moieties and endotoxins (Suwan et al. 2012; Azurmendi et al. 2020). Sensitive analytical methods are required to analyze for the presence of unnatural sugar moieties in heparosan (Datta et al. 2020), and ongoing improvements in chemical removal of process impurities from *E. coli*-derived products are needed (Whitfield 2006; Suwan et al. 2012; Lodowska et al. 2013; Qiao et al. 2020; Azurmendi et al. 2020).

With similar fermentation and purification conditions, the yield of Nissle-derived heparosan is considerably lower than *E. coli* K5-derived heparosan (Table S4). The heparosan yield from the Nissle 1917 strain may be further improved through additional optimization of fermentation conditions and through metabolic engineering strategies (Hobbs and Reeves 1994; Xue et al. 2009). For example, it has been demonstrated that a mutation or deletion of the *waaR* gene (lipopolysaccharide 1,2-glucosyltransferase gene) may result in (1) disruption of lipopolysaccharide outer core biosynthesis and cell surface retention of group 2 polysaccharides (Taylor et al. 2006), and (2) under certain fermentation conditions, may result in the decrease in the MW of the heparosan (Huang et al. 2016). Unfortunately, genetic engineering would result in a GMO that could lead to adverse market acceptability in functional food and nutraceutical applications. The feasibility to biomanufacture heparosan in a BSL-1 facility may have a significant impact in reducing heparosan production costs. The study successfully reports high cell density fermentation of probiotic bacteria EcN (*E. coli* Nissle 1917), using a chemically defined media. Production of unimodal heparosan chains is a desirable quality for downstream processing and applications. The current work also demonstrates the process parameters towards the production of monodispersed heparosan using probiotic bacteria EcN (Nissle 1917).

Supplementary Information The online version contains supplementary material available at https://doi.org/10.1007/s00253-020-11079-9.

Authors' contributions RJL and JSD provided the funding for this study. PD, RJL, and JSD planned the study and wrote the manuscript. PD was responsible for the upstream processing and analysis studies. LF and BP were responsible for the downstream processing and analysis studies.

Funding This research was sponsored by the National Institutes of Health grant #CA231074.

Data availability The strains used in the manuscript have been described previously and referenced in the manuscript. The annotated draft genome sequence of *E. coli* K5 (*Escherichia coli* Strain ATCC 23506, Serovar O10:K5:H4) has been deposited in DDBJ/EMBL/GenBank previously under the accession no. CAPK00000000 (https://www.ncbi.nlm.nih.gov/nuccore/CAPK00000000.1). The annotated draft genome sequence of *E. coli* Nissle 1917 (*Escherichia coli* Strain Nissle 1917, Serovar O6:K5:H1) has been deposited in DDBJ/EMBL/GenBank previously under the accession no. CAPM00000000 (https://www.ncbi.nlm.nih.gov/nuccore/CAPM00000000.1).

Compliance with ethical standards

This article does not contain any studies with human participants or animals performed by any of the authors.

Conflict of interest The authors declare that they have no conflict of interest.

References

Azurmendi HF, Veeramachineni V, Freese S, Lichaa F, Freedberg DI, Vann WF (2020) Chemical structure and genetic organization of the *E. coli* O6:K15 capsular polysaccharide. Sci Rep 10:12608 . https://doi.org/10.1038/s41598-020-69476-z

Chen X, Chen R, Yu X, Tang D, Yao W, Gao X (2017) Metabolic engineering of *Bacillus subtilis* for biosynthesis of heparosan using heparosan synthase from Pasteurella multocida, PmHS1. Bioprocess Biosyst Eng 40:675–681. https://doi.org/10.1007/s00449-016-1732-4

Corbett D, Bennett HJ, Askar H, Green J, Roberts IS (2007) SlyA and H-NS regulate transcription of the *Escherichia coli* K5 capsule gene cluster, and expression of slyA in *Escherichia coli* is temperature-dependent, positively autoregulated, and independent of H-NS. J Biol Chem 282:33326–33335. https://doi.org/10.1074/jbc.M703465200

Cress BF, Erkert KA, Barquera B, Koffas MAG (2013a) Draft genome sequence of *Escherichia coli* strain ATCC 23506 (serovar O10:K5:H4). Genome Announc 1:(2):e0004913 . https://doi.org/10.1128/genomeA.00049-13

Cress BF, Linhardt RJ, Koffas MAG (2013b) Draft genome sequence of *Escherichia coli* strain Nissle 1917 (serovar O6:K5:H1). Genome Announc 1(2):e00047–e00013. https://doi.org/10.1128/genomeA.00047-13

Cress BF, Englaender JA, He W, Kasper D, Linhardt RJ, Koffas MAG (2014) Masquerading microbial pathogens: capsular polysaccharides mimic host-tissue molecules. FEMS Microbiol Rev 38:660–697

Datta P, Li G, Yang B, Zhao X, Baik JY, Gemmill TR, Sharfstein ST, Linhardt RJ (2013) Bioengineered Chinese hamster ovary cells with golgi-targeted 3-O-sulfotransferase-1 biosynthesize heparan sulfate with an antithrombin-binding site. J Biol Chem 288:37308–37318. https://doi.org/10.1074/jbc.M113.519033

Datta P, Yan L, Awofiranye A, Dordick JS, Linhardt RJ (2020) Heparosan chain characterization: sequential depolymerization of *E. coli* K5 heparosan by a bacterial eliminase heparin lyase III and a bacterial hydrolase heparanase Bp to prepare defined oligomers. Biotechnol J 2000336 . doi:https://doi.org/10.1002/biot.202000336

Deangelis PL (2015) Heparosan, a promising "naturally good" polymeric conjugating vehicle for delivery of injectable therapeutics. Expert Opin Drug Deliv 12:349–352

DeAngelis PL, White CL (2002) Identification and molecular cloning of a heparosan synthase from *Pasteurella multocida* type D. J Biol Chem 277:7209–7213. https://doi.org/10.1074/jbc.M112130200

Fu L, Suflita M, Linhardt RJ (2016) Bioengineered heparins and heparan sulfates. Adv Drug Deliv Rev 97:237–249. https://doi.org/10.1016/j.addr.2015.11.002

Fu L, Li K, Mori D, Hirakane M, Lin L, Grover N, Datta P, Yu Y, Zhao J, Zhang F, Yalcin M, Mousa SA, Dordick JS, Linhardt RJ (2017) Enzymatic generation of highly anticoagulant bovine intestinal heparin. J Med Chem 60:8673–8679. https://doi.org/10.1021/acs.jmedchem.7b01269

Hobbs M, Reeves PR (1994) The JUMPstart sequence: a 39 bp element common to several polysaccharide gene clusters. Mol Microbiol 12:855–856. https://doi.org/10.1111/j.1365-2958.1994.tb01071.x

Huang H, Liu X, Lv S, Zhong W, Zhang F, Linhardt RJ (2016) Recombinant *Escherichia coli* K5 strain with the deletion of waaR gene decreases the molecular weight of the heparosan capsular polysaccharide. Appl Microbiol Biotechnol 100:7877–7885. https://doi.org/10.1007/s00253-016-7511-y

Kim SY, Jin W, Sood A, Montgomery DW, Grant OC, Fuster MM, Fu L, Dordick JS, Woods RJ, Zhang F, Linhardt RJ (2020) Characterization of heparin and severe acute respiratory syndrome-related coronavirus 2 (SARS-CoV-2) spike glycoprotein binding interactions. Antivir Res 181:104873. https://doi.org/10.1016/j.antiviral.2020.104873

Lee SY (1996) High cell-density culture of *Escherichia coli*. Trends Biotechnol 14:98–105

Lindahl U, Kusche-Gullberg M, Kjellen L (1998) Regulated diversity of heparan sulfate. J Biol Chem 273:24979–24982

Lindahl U, Li JP, Kusche-Gullberg M, Salmivirta M, Alaranta S, Veromaa T, Emeis J, Roberts I, Taylor C, Oreste P, Zoppetti G, Naggi A, Torri G, Casu B (2005) Generation of "neoheparin" from *E. coli* K5 capsular polysaccharide. J Med Chem 48:349–352. https://doi.org/10.1021/jm049812m

Linhardt RJ (2003) 2003 Claude S. Hudson award address in carbohydrate chemistry. Heparin: Structure and activity. J Med Chem 46:2551–2564 . https://doi.org/10.1021/jm030176m

Linhardt RJ, Toida T (2004) Role of glycosaminoglycans in cellular communication. Acc Chem Res 37:431–438. https://doi.org/10.1021/ar030138x

Linhardt RJ, Dordick JS, Deangelis PL, Liu J (2007) Enzymatic synthesis of glycosaminoglycan heparin. In: Seminars in Thrombosis and Hemostasis. Copyright © 2007 by Thieme Medical Publishers, Inc., 333 Seventh Avenue, New York, NY 10001, USA., pp 453–465

Liu J, Linhardt RJ (2014) Chemoenzymatic synthesis of heparan sulfate and heparin. Nat Prod Rep 31:1676–1685. https://doi.org/10.1039/c4np00076e

Lodowska J, Wolny D, Weglarz L (2013) The sugar 3-deoxy-D-manno-oct-2-ulosonic acid (Kdo) as a characteristic component of bacterial endotoxin - a review of its biosynthesis, function, and placement in the lipopolysaccharide core. Can J Microbiol 59:645–655

Ly M, Wang Z, Laremore TN, Zhang F, Zhong W, Pu D, Zagorevski DV, Dordick JS, Linhardt RJ (2011) Analysis of *E. coli* K5 capsular polysaccharide heparosan. Anal Bioanal Chem 399:737–745. https://doi.org/10.1007/s00216-010-3679-7

Meyer H-P, Minas W, Schmidhalter D (2016) Industrial-scale fermentation. In: Industrial biotechnology. Wiley-VCH Verlag GmbH & Co. KGaA, Weinheim, pp 1–53

Phue J-N, Shiloach J (2004) Transcription levels of key metabolic genes are the cause for different glucose utilization pathways in *E. coli* B (BL21) and *E. coli* K (JM109). J Biotechnol 109:21–30. https://doi.org/10.1016/j.jbiotec.2003.10.038

Qiao M, Lin L, Xia K, Li J, Zhang X, Linhardt RJ (2020) Recent advances in biotechnology for heparin and heparan sulfate analysis. Talanta 219:121270. https://doi.org/10.1016/j.talanta.2020.121270

Qiu L, Shan X, Long M, Ahmed KS, Zhao L, Mao J, Zhang H, Sun C, You C, Lv G, Chen J (2019) Elucidation of cellular uptake and intracellular trafficking of heparosan polysaccharide-based micelles in various cancer cells. Int J Biol Macromol 130:755–764. https://doi.org/10.1016/j.ijbiomac.2019.02.133

Restaino OF, Cimini D, De Rosa M, Catapano A, De Rosa M, Schiraldi C (2011) High cell density cultivation of *Escherichia coli* K4 in a microfiltration bioreactor: a step towards improvement of chondroitin precursor production. Microb Cell Factories 10:1–10. https://doi.org/10.1186/1475-2859-10-10

Restaino OF, D'ambrosio S, Cassese E, Ferraiuolo SB, Alfano A, Ventriglia R, Marrazzo A, Schiraldi C, Cimini D (2019) Molecular weight determination of heparosan- and chondroitin-like capsular polysaccharides: figuring out differences between wild-type and engineered *Escherichia coli* strains. Appl Microbiol Biotechnol 103:6771–6782. https://doi.org/10.1007/s00253-019-09969-8

Rippe M, Stefanello TF, Kaplum V, Britta EA, Garcia FP, Poirot R, Companhoni MVP, Nakamura CV, Szarpak-Jankowska A, Auzély-Velty R (2019) Heparosan as a potential alternative to hyaluronic acid for the design of biopolymer-based nanovectors for anticancer therapy. Biomater Sci 7:2850–2860. https://doi.org/10.1039/c9bm00443b

Rowe S, Hodson N, Griffiths G, Roberts IS (2000) Regulation of the *Escherichia coli* K5 capsule gene cluster: evidence for the roles of H-NS, BipA, and integration host factor in regulation of group 2 capsule gene clusters in pathogenic *E. coli*. J Bacteriol 182:2741–2745. https://doi.org/10.1128/JB.182.10.2741-2745.2000

Soares da Costa D, Reis RL, Pashkuleva I (2017) Sulfation of glycosaminoglycans and its implications in human health and disorders. Annu Rev Biomed Eng 19:1–26. https://doi.org/10.1146/annurev-bioeng-071516-044610

Suwan J, Torelli A, Onishi A, Dordick JS, Linhardt RJ (2012) Addressing endotoxin issues in bioengineered heparin. Biotechnol Appl Biochem 59:420–428. https://doi.org/10.1002/bab.1042

Taylor CM, Goldrick M, Lord L, Roberts IS (2006) Mutations in the waaR gene of *Escherichia coli* which disrupt lipopolysaccharide outer core biosynthesis affect cell surface retention of group 2 capsular polysaccharides. J Bacteriol 188:1165–1168. https://doi.org/10.1128/JB.188.3.1165-1168.2006

Vann WF, Schmidt MA, Jann B, Jann K (1981) The structure of the capsular polysaccharide (K5 Antigen) of urinary-tract-infective *Escherichia coli* 010:K5:H4: a polymer similar to desulfo-heparin. Eur J Biochem 116:359–364. https://doi.org/10.1111/j.1432-1033.1981.tb05343.x

Wang Z, Ly M, Zhang F, Zhong W, Suen A, Hickey AM, Dordick JS, Linhardt RJ (2010) *E. coli* K5 fermentation and the preparation of heparosan, a bioengineered heparin precursor. Biotechnol Bioeng 107:964–973. https://doi.org/10.1002/bit.22898

Wang Z, Yang B, Zhang Z, Ly M, Takieddin M, Mousa S, Liu J, Dordick JS, Linhardt RJ (2011) Control of the heparosan N-deacetylation leads to an improved bioengineered heparin. Appl Microbiol Biotechnol 91:91–99. https://doi.org/10.1007/s00253-011-3231-5

Wang Z, Linhardt RJ, Dordick JS, Bhaskar U (2014) K5 heparosan fermentation and purification. US Pat #8,883,452

Wang T, Liu L, Voglmeir J (2020) Chemoenzymatic synthesis of ultra-low and low-molecular weight heparins. Biochim Biophys Acta - Proteins Proteomics 1868:140301. https://doi.org/10.1016/j.bbapap.2019.140301

Whitfield C (2006) Biosynthesis and assembly of capsular polysaccharides in *Escherichia coli*. Annu Rev Biochem 75:39–68. https://doi.org/10.1146/annurev.biochem.75.103004.142545

Williams A, Gedeon KS, Vaidyanathan D, Yu Y, Collins CH, Dordick JS, Linhardt RJ, Koffas MAG (2019) Metabolic engineering of *Bacillus megaterium* for heparosan biosynthesis using Pasteurella multocida heparosan synthase, PmHS2. Microb Cell Factories 18:132. https://doi.org/10.1186/s12934-019-1187-9

Xu Y, Masuko S, Takieddin M, Xu H, Liu R, Jing J, Mousa SA, Linhardt RJ, Liu J (2011) Chemoenzymatic synthesis of homogeneous ultra-low molecular weight heparins. Science (80-) 334:498–501 . https://doi.org/10.1126/science.1207478

Xue P, Corbett D, Goldrick M, Naylor C, Roberts IS (2009) Regulation of expression of the region 3 promoter of the *Escherichia coli* K5 capsule gene cluster involves H-NS, SlyA, and a large 5′ untranslated region7. J Bacteriol 191:1838–1846. https://doi.org/10.1128/JB.01388-08

Yamazaki S, Shimizu T, Mori K, Tonouchi N (2020) Heparosan producing bacterium and heparosan manufacturing method. US Pat #10,611,804 US Pat. #10,611,804

Yan H, Bao F, Zhao L, Yu Y, Tang J, Zhou X (2015) Cyclic AMP (cAMP) receptor protein-cAMP complex regulates heparosan production in *Escherichia coli* strain Nissle 1917. Appl Environ Microbiol 81:7687–7696. https://doi.org/10.1128/AEM.01814-15

Yang B, Solakyildirim K, Chang Y, Linhardt RJ (2011) Hyphenated techniques for the analysis of heparin and heparan sulfate. Anal Bioanal Chem 399:541–557

Zhang F, Zhang Z, Linhardt RJ (2010) Glycosaminoglycans. Handbook of Glycomics. Elsevier Inc., In, pp 59–80

Zhang F, Yang B, Ly M, Solakyildirim K, Xiao Z, Wang Z, Beaudet JM, Torelli AY, Dordick JS, Linhardt RJ (2011) Structural characterization of heparins from different commercial sources. Analytical and Bioanalytical Chemistry. Springer, In, pp 2793–2803

Zhang C, Liu L, Teng L, Chen J, Liu J, Li J, Du G, Chen J (2012) Metabolic engineering of *Escherichia coli* BL21 for biosynthesis of heparosan, a bioengineered heparin precursor. Metab Eng 14:521–527. https://doi.org/10.1016/j.ymben.2012.06.005

Zhang X, Lin L, Huang H, Linhardt RJ (2020) Chemoenzymatic synthesis of Glycosaminoglycans. Acc Chem Res 53:335–346. https://doi.org/10.1021/acs.accounts.9b00420

Zhao X, Yang B, Datta P, Gasmili L, Zhang F, Linhardt RJ (2012) Cell-based microscale isolation of glycoaminoglycans for glycomics study. J Carbohydr Chem 31:420–435. https://doi.org/10.1080/07328303.2012.658126

Zhao X, Yang B, Linkens K, Datta P, Onishi A, Zhang F, Linhardt RJ (2013) Microscale separation of heparosan, heparan sulfate, and heparin. Anal Biochem 434:215–217. https://doi.org/10.1016/j.ab.2012.12.009